

Article

Culture of *Mycobacterium smegmatis* in Different Carbon Sources to Induce In Vitro Cholesterol Consumption Leads to Alterations in the Host Cells after Infection: A Macrophage Proteomics Analysis

Jaqueline Batista de Lima ^{1,2}, Lana Patricia da Silva Fonseca ³, Luciana Pereira Xavier ², Barbarella de Matos Macchi ^{4,5}, Juliana Silva Cassoli ⁶, Edilene Oliveira da Silva ^{1,7} , Rafael Borges da Silva Valadares ³ , José Luiz Martins do Nascimento ^{4,5}, Agenor Valadares Santos ² and Chubert Bernardo Castro de Sena ^{1,5,*} 

- ¹ Laboratory of Structural Biology, Institute of Biological Sciences, Federal University of Pará, Belém 66075-110, PA, Brazil; jaqueline.lima@icb.ufpa.br (J.B.d.L.); edilene@ufpa.br (E.O.d.S.)
- ² Laboratory of Biotechnology of Enzymes and Biotransformations, Institute of Biological Sciences, Federal University of Pará, Belém 66075-110, PA, Brazil; lpxavier@ufpa.br (L.P.X.); avsantos@ufpa.br (A.V.S.)
- ³ Instituto Tecnológico Vale, Belém 66055-090, PA, Brazil; lanafonseca@ufrn.edu.br (L.P.d.S.F.); Rafael.borges.valadares@itv.org (R.B.d.S.V.)
- ⁴ Laboratory of Molecular and Cellular Neurochemistry, Institute of Biological Sciences, Federal University of Pará, Belém 66075-110, PA, Brazil; barbarella@ufpa.br (B.d.M.M.); jlmn@ufpa.br (J.L.M.d.N.)
- ⁵ National Institute of Science and Technology in Neuroimmunomodulation (INCT-NIM), Rio de Janeiro 21040-900, RJ, Brazil
- ⁶ Institute of Biological Sciences, Federal University of Pará, Belém 66075-110, PA, Brazil; jscassoli@ufpa.br
- ⁷ National Institute of Science and Technology in Structural Biology and Bioimaging, Rio de Janeiro 21941-901, RJ, Brazil
- * Correspondence: chubert@ufpa.br



Citation: de Lima, J.B.; da Silva Fonseca, L.P.; Xavier, L.P.; de Matos Macchi, B.; Cassoli, J.S.; da Silva, E.O.; da Silva Valadares, R.B.; do Nascimento, J.L.M.; Santos, A.V.; de Sena, C.B.C. Culture of *Mycobacterium smegmatis* in Different Carbon Sources to Induce In Vitro Cholesterol Consumption Leads to Alterations in the Host Cells after Infection: A Macrophage Proteomics Analysis. *Pathogens* **2021**, *10*, 662. <https://doi.org/10.3390/pathogens10060662>

Academic Editor: Jean-Pierre Gorvel

Received: 30 April 2021

Accepted: 26 May 2021

Published: 28 May 2021

Publisher's Note: MDPI stays neutral with regard to jurisdictional claims in published maps and institutional affiliations.



Copyright: © 2021 by the authors. Licensee MDPI, Basel, Switzerland. This article is an open access article distributed under the terms and conditions of the Creative Commons Attribution (CC BY) license (<https://creativecommons.org/licenses/by/4.0/>).

Abstract: During tuberculosis, *Mycobacterium* uses host macrophage cholesterol as a carbon and energy source. To mimic these conditions, *Mycobacterium smegmatis* can be cultured in minimal medium (MM) to induce cholesterol consumption in vitro. During cultivation, *M. smegmatis* consumes MM cholesterol and changes the accumulation of cell wall compounds, such as PIMs, LM, and LAM, which plays an important role in its pathogenicity. These changes lead to cell surface hydrophobicity modifications and H₂O₂ susceptibility. Furthermore, when *M. smegmatis* infects J774A.1 macrophages, it induces granuloma-like structure formation. The present study aims to assess macrophage molecular disturbances caused by *M. smegmatis* after cholesterol consumption, using proteomics analyses. Proteins that showed changes in expression levels were analyzed in silico using OmicsBox and String analysis to investigate the canonical pathways and functional networks involved in infection. Our results demonstrate that, after cholesterol consumption, *M. smegmatis* can induce deregulation of protein expression in macrophages. Many of these proteins are related to cytoskeleton remodeling, immune response, the ubiquitination pathway, mRNA processing, and immunometabolism. The identification of these proteins sheds light on the biochemical pathways involved in the mechanisms of action of mycobacteria infection, and may suggest novel protein targets for the development of new and improved treatments.

Keywords: *Mycobacterium*; proteomics; cholesterol; infection; macrophages

1. Introduction

Tuberculosis (TB) is a communicable disease that is a major cause of ill health worldwide. A quarter of the global population is infected with the causative agent, *Mycobacterium tuberculosis* (*M. tuberculosis*), and thus at risk of developing TB disease. It is estimated that

1.2 million people died of TB in 2019 [1]. TB is transmitted by aerosols in droplets containing the bacteria from an infected individual to a healthy individual. The improvement of knowledge regarding the host–pathogen interaction is one manner of overcoming obstacles to control TB.

M. tuberculosis is a successful human pathogen that is able to grow and replicate within a host and its success as an infectious agent is due, in large, to its ability to persist in the macrophages [2]. The pathogenesis of tuberculosis is controlled by a complex interaction between the host immune system and survival strategies developed by *M. tuberculosis* [2].

Alveolar macrophages are the most important immune cell defense against *M. tuberculosis* and, in addition to inducing the innate immune response, they also play central roles in TB control. These cells recognize and phagocytose pathogens, such as *M. tuberculosis*, which resides in a membrane-bound vacuole inside the host, the phagosome, which usually matures into phagolysosomes. Other mechanisms employed to kill *M. tuberculosis* include the production of reactive oxygen and nitrogen intermediates, cytokine generation, up regulation of the expression of antimicrobial peptides, classical killing pathways such as autophagy and apoptosis, lipid mediator release, and sequestration of cofactors. Disruption of any of these macrophage functions affects the immune response [3,4].

Although macrophages are thought to be an effective barrier against pathogens, *M. tuberculosis* has evolved mechanisms to evade the host immune response, thereby creating a favorable environment for intracellular replication via the exploitation of cell wall components such as phosphatidylinositol mannosides (PIMs), lipomannan (LM), lipoarabinomannan (LAM), trehalose dimycolate (TDM), glycopeptidolipid (GPL), and mycolic acids. All of these compounds are key modulators of host immune processes and leads to the inhibition of phagosome-lysosome fusion and phagosome acidification, the modulation of macrophage membrane properties and the host cell cytoskeleton, as well as host cell signaling inhibition, programmed death mechanisms, downregulation of host gene expression, and formation of granuloma [3,5–9].

Many of these processes are modified by *M. tuberculosis*, which causes inhibition, activation, recruitment, retention, or accumulation of several proteins as a strategy for survival in the hostile environment of the host. Some of these proteins are TACO/coronin-1 which is recruited and retained to block phagosome-lysosome fusion, calcineurin that also contributes to blocking phagosome-lysosome fusion, v-ATPase whose exclusion inhibits phagosome acidification, and many others [10]. In contrast, non-pathogenic mycobacteria, such as *Mycobacterium smegmatis*, reside in phagosomes that are fully mature by fusing with late endocytic compartments, a process that facilitates the killing of these bacteria [11,12]. An emerging topic in TB pathogenesis is the manipulation of host lipid metabolism by *M. tuberculosis*, whereby fatty acids and cholesterol are routed toward intracellular bacilli. Inside the phagosome, *M. tuberculosis* requires host lipids and cholesterol to accumulate lipid droplets and induce foamy macrophages. Host cholesterol has already been shown to be required for optimal growth and persistence of *M. tuberculosis* during infection, where the bacterium uses it as a source of carbon and biosynthetic precursors that are needed to produce virulence-associated molecules [2,13–15].

In a recent study by our research group, Santos et al. (2019) [16] provided the first evidence that the culture of non-pathogenic *M. smegmatis* in minimal medium (MM) to induce cholesterol consumption leads to several changes in the bacterial cell wall structure. The authors demonstrated that cholesterol availability in MM doubled the amount of intracellular cholesterol, only when glycerol is lacking, showing it to be important for the maintenance of small lipids such as PIMs and phospholipids on the mycobacterial surface. Moreover, *M. smegmatis* also grows in MM, independently of the presence of cholesterol, where it is induced to use mycolic acids to maintain TDM levels, thereby decreasing cell wall mycolate accumulation. In addition to depleting mycolic acid contents in the cell wall, *M. smegmatis* also changes the biosynthesis of LM and LAM, generating unusual molecules. This report demonstrated the importance of mycolic acids and LM and LAM for maintaining the integrity of the *M. smegmatis* cell wall after culturing in

minimal growth conditions similar to those occurring in macrophage infection, where bacteria must induce the accumulation of host cholesterol to survive [13,14,17]. In the same work, in response to the new environment and after mycolic acid reduction, GPLs were highly present and were necessary to maintain the integrity of the cell wall and ensure cell survival after culture in MM. All these changes help mycobacteria to modify cell surface hydrophobicity and become resistant to hydrogen peroxide. It is possible that this new MM environment can change the physiology of the mycobacteria to allow the bacilli to become resistant to phagocytosis. In addition, following cell wall modifications, the infection of J774A.1 macrophages with *M. smegmatis*, the host changes its cellular reorganization to form granuloma-like structures. In particular, the high quantities of these structures show that the use of cholesterol by non-pathogenic *M. smegmatis* can potentiate the infection by this mycobacteria [16].

Recently, a number of proteomics researchers have reported the deregulation of several proteins during host–pathogen interactions induced by *M. tuberculosis*, indicating significant changes in biological processes such as apoptosis, blood coagulation, and oxidative phosphorylation [18]. A variety of studies have investigated cells stimulated by infection or mycobacterial bioactive lipids [18–22]. One study showed that the infection of macrophages with mycobacterial cell wall lipids altered the differential expression of proteins involved in immune response, oxidation and reduction, and vesicle transport, as well as other cellular processes [19].

Here, for the first time, using a proteomic study, we show that the infection of macrophages with a fast-growing and non-pathogenic bacterium, *M. smegmatis*, led to several changes in the differential expression of numerous proteins after induction of cholesterol consumption and consequent infection.

2. Materials and Methods

2.1. Mycobacterial Strain and Culture Conditions

Mycobacterium smegmatis (Trevisan) of the Lehmann and Neumann strain (American Type Culture Collection, ATCC 607; Instituto Nacional de Controle de Qualidade em Saúde, INCQS 00021) were kindly provided by Fundação Oswaldo Cruz-FIOCRUZ, Rio de Janeiro, RJ, Brazil. For each experiment, the strain was grown on Middlebrook 7H10 agar supplemented with 0.5% glycerol, 0.2% glucose, and 14 mM NaCl at 37 °C for 3 days. After this time, cells were cultured until late stationary growth phase in Middlebrook 7H9 broth (BD Biosciences) supplemented with 0.2% glycerol, 0.2% glucose, 0.05% tyloxapol, and 14 mM NaCl at 37 °C for 3 days with agitation at 250 r.p.m [23]. The bacterial culture in the stationary phase of growth was diluted for new 20 mL culture with OD₆₀₀ 0.05 in fresh Middlebrook 7H9 broth or in minimal media (MM) containing compounds like ZnSO₄ (0.1 mg/L), MgSO₄·7H₂O (0.5 g/L), Na₂HPO₄ (2.5 g/L), CaCl₂ (0.5 g/L), KH₂PO₄ (1.0 g/L), NH₄Fe(SO₄)₂·12H₂O (50 mg/L), asparagine (0.5 g/L), vitamin B12 (10 mg/mL), 0.2% tyloxapol, and 0.1% glycerol (in 7H9) or 0.01% cholesterol [14]. The cells were cultured in three groups: (1) 7H9 + Gly (Middlebrook 7H9 broth supplemented with glycerol); (2) MM + Chol (minimal medium supplemented with cholesterol); and (3) MM (only minimal medium). The optical density at 600 nm (A₆₀₀) was used to analyze the bacterial growth [16].

2.2. Macrophage Culture and Infection with *Mycobacterium Smegmatis*

The J774A.1 cells (ATCC TIB-67, Cell Bank of Rio de Janeiro–BCRJ, Rio de Janeiro, RJ, Brazil), a murine macrophage cell line, was cultured in DMEM medium with 10% fetal bovine serum, 100 U/mL penicillin, and 100 µg/mL streptomycin. The cells were maintained at 37 °C in a 5% CO₂-humidified atmosphere. For infection, macrophages cells (6.6 × 10⁵/flask) were seeded in cell culture flasks and incubated for 2 days until reaching 90% confluence. Bacterial cultures at the early stationary phase were pelleted, washed twice in PBS pH 7.4, bath-sonicated for 15 min to disrupt bacterial clumps, and resuspended in DMEM medium to a final OD₆₀₀ 0.1. Macrophages were infected with *M.*

M. smegmatis (grown in three different bacterial culture mediums) at a multiplicity of infection (MOI) of 100:1. In each experiment, after 1 h infection, extracellular bacteria were dead after addition of 10 µg/mL gentamicin. After 12 h of infection, the cells were washed three times with cold PBS pH 7.4 [11,16]. Macrophages without infection were used as a control group as shown in Figure 1.

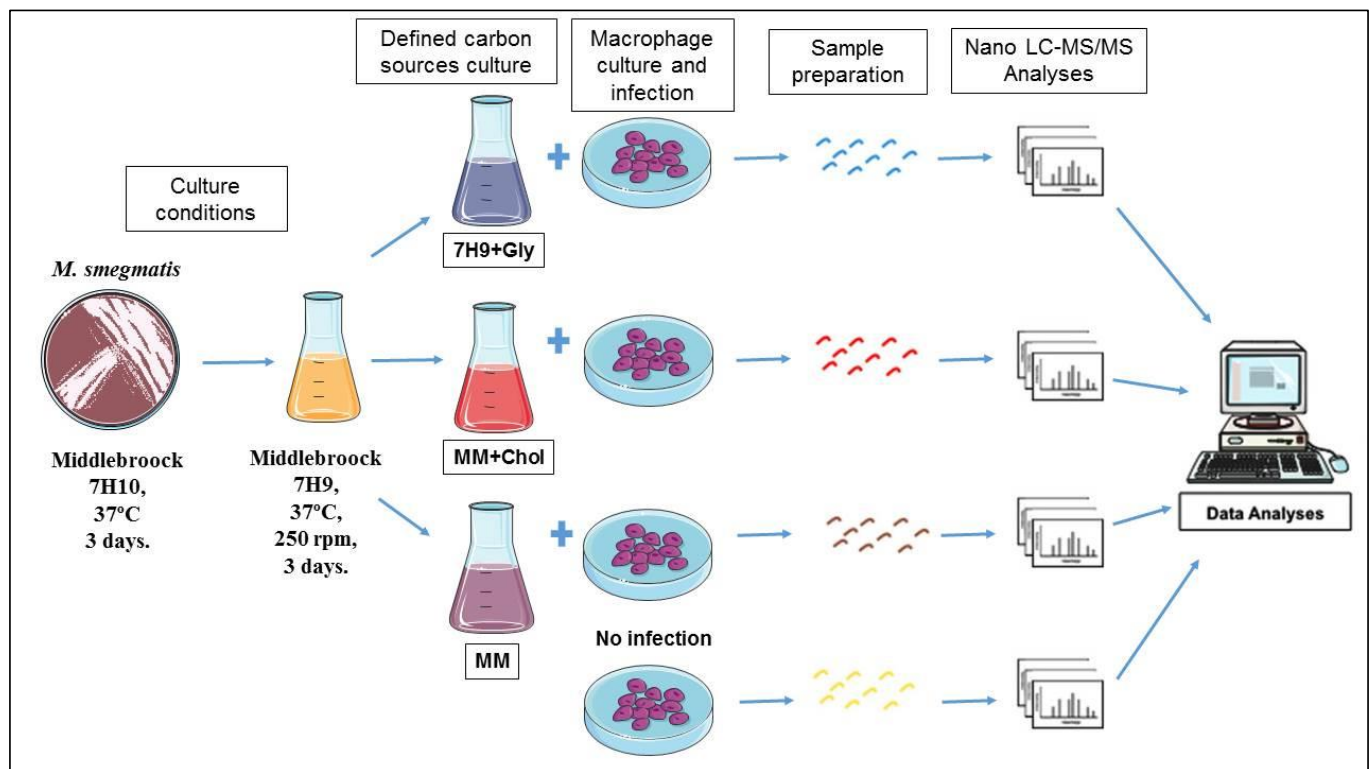


Figure 1. Experimental design. The macrophage cell line J774A.1 was cultivated and infected with *M. smegmatis* grown in different nutritional conditions. Proteins were extracted and analyzed by Nano-LC-ESI MS/MS. As a control, uninfected macrophages were used.

2.3. Cell Lysis and Sample Preparation

After 12 h of infection, the cells were washed with cold PBS pH 7.4 (three times) and harvested by scraping in PBS. Cells were centrifuged at $1500\times g$ for 5 min on ice and resuspended in 6 M urea, 2 M thiourea, and 10 mM dithiothreitol (DTT) for lysis and reduction for 2 h at 37 °C. After incubation, the samples were diluted 10-folds in 20 mM ammonium bicarbonate pH 7.5 and sonicated on ice. For alkylation, 200 mM of iodoacetamide in 20 mM of triethylammonium bicarbonate (to achieve a final concentration of 20 mM iodoacetamide) was added and incubated for 20 min in the dark at room temperature, to reduce and alkylate cysteine residues. Protein concentrations were measured using the Qubit Protein Assay Kit (Invitrogen). The samples were digested with trypsin at 1:50 (*w:w*; trypsin:sample) and incubated at 37 °C overnight. The digestion process was stopped by adding 10 µL of 5% trifluoroacetic acid (TFA) [24].

The samples were desalted using a C18 column (SepPack 50 ng Waters), assembling a vacuum system with manifold (Waters) and vacuum pump (Millipore). The column was activated with 100% acetonitrile (ACN), equilibrated with 50% ACN on 0.1% formic acid (FA), and equilibrated again with 1 mL of 0.1% TFA. The sample was previously acidified with 0.4% TFA, loaded onto C18, and the salt removed from the sample with 0.1% TFA. The column was equilibrated again with FA. The sample was eluted with 50% ACN on 0.1% FA, and 80% CAN on 0.1% FA. The samples were concentrated in a SpeedVac evaporator

at 25 °C for 24 h, and resuspended in 20 mM ammonium formate, diluted 10 times, in the proportion of 75 µL for each 50 ng of protein in the samples [24].

2.4. NanoLC-ESI MS/MS Analysis

Proteomic analysis was performed in a bidimensional nanoUPLC tandem nanoESI-MS/MS platform and the MS/MS fragmentation spectra were acquired in multiplexed data-independent mode (MSE) using a 2D-RP/RP Nano Acquity UPLC System (Waters Corporation, Milford, MA, USA) coupled to a Synapt G2 mass spectrometer (Waters Corporation, Milford, MA, USA). One-dimension reversed-phase (RP) approach was used to fractionate the samples. Peptide samples (0.5 µg) were loaded onto an Acquity UPLC M-Class CSH (C18 packed with changed surface hybrid) Column (100 Å, 1.8 µm, 100 µm × 100 mm; Waters Corporation, Milford, MA, USA) at a flow rate of 2 µL/min. An acetonitrile gradient from 3% to 40% *v/v* at flow rate 400 nL/min⁻¹ for 40 min was used for peptide fractionation directly into a Synapt G2. The mass spectrometer was operated in the resolution mode with an *m/z* resolving power of about 20,000 FWHM for every measurement. MS and MS/MS data were acquired in positive ion mode in the range of 50–1200 *m/z*. The low-energy MS mode by applying constant collision energy of 4 eV was used to collect precursor ion information, and the elevated energy scan using a ramped collision energy (19–45 eV) applied to the collision-induced dissociation cell was used to fragment ion information. The lock mass channel was sampled every 30 sec using 0.1 s scans over the same mass range. For mass spectrometer calibration was used an MS/MS spectrum of [Glu¹]-Fibrinopeptide B human (785.8426 *m/z*) solution that was delivered through the reference sprayer of the NanoLock Spray source [25].

2.5. Data Processing and Database Searches

For identification and quantification of proteins, were used dedicated algorithms and searching against the UniProt Proteomic Database of *Mus musculus*, version 2019/06 (55,197 proteins) [24,26]. To assess the false-positive identification rate, the databases used were reversed “on the fly” during database queries by the software. We used the Progenesis QI for Proteomics software package with Apex3D, Peptide 3D, and Ion Accounting informatics (Waters Corporation) for correct spectral processing and database searching conditions. This software loads the LC-MS data, followed by alignment and peak detection, which creates a list of relevant peptide ions that are analyzed within Peptide Ion Stats by multivariate statistical methods. The processing parameters used were 500 counts for the low-energy threshold and 50.0 counts for the elevated energy threshold. For the processing, all runs in the experiment were automatically aligned and assessed for suitability. For peak picking, eight was used as the maximum ion charge and the sensitivity value was selected as four. In addition, some parameters were considered in the identification of proteins/peptides: (1) digestion by trypsin with at most two missed cleavages; (2) variable modification by oxidation and fixed modification by carbamidomethyl; and (3) a false discovery rate (FDR) of less than 1%. For ion matching, the following were required: two or more ion fragments per peptide, five or more fragments per protein, and one or more peptides per protein. Data were analyzed by one-way analysis of variance (ANOVA) with treatment factor *p*-value < 0.05 compared to the vehicle group, and identifications that were outside these criteria were rejected. The label free protein quantitation was performed using the Hi-N (N = 3) method because the experimental design was defined in 3 groups (1–3 groups). Ratios between the mean values of protein abundances from treated groups, over the mean values of protein abundances from the control group, were calculated for each protein. Proteins which had expression 1.0-fold (log₂ fold) increased or decreased in treated groups in comparison to the control group were considered up- or down-regulated.

2.6. Functional Correlation Analysis

For interpretation of the functional significance of identified and quantified proteins, gene ontology annotations were performed using Blast2GO Annotation using OmicsBox

software. STRING v.11 was used to determine potential interactions between proteins from experimental groups and also between these proteins and other proteins from the STRING database. The Venn diagram was drawn using Draw Venn Diagram Online.

3. Results and Discussion

3.1. Proteomics Revealed Different Expression Profiles When Macrophages Are Infected with *M. smegmatis* after Cholesterol Consumption

To study the effects of different nutritional sources provided to *M. smegmatis* when infecting macrophages, proteome proteins were analyzed by Nano-LC-ESI MS/MS. For this, mycobacteria were cultivated under three different conditions and used for infection experiments: (1) *M. smegmatis* cultivated in complete medium Middlebrook 7H9 broth, which is normally supplemented with glycerol (7H9 + Gly); (2) culture in MM with cholesterol supplementation (MM + Chol); and (3) culture in MM without supplementation (MM). Macrophage proteins were extracted at 12 h after infection with the mycobacterial groups. Macrophages without infection were used as a control group (Figure 1). As a result, a total of 1265 proteins were identified in three independent experiments, among them, 614 were distinct proteins. The mass spectrometry proteomics data were deposited in the ProteomeXchange Consortium via the PRIDE partner repository, with the dataset identifier PXD025783 [27–29]. Data demonstrated 90, 58, and 91 exclusive proteins in 7H9 + Gly, MM + Chol, and MM, respectively. The three groups had 276 proteins in common, as shown in the Venn diagram, Figure 2.

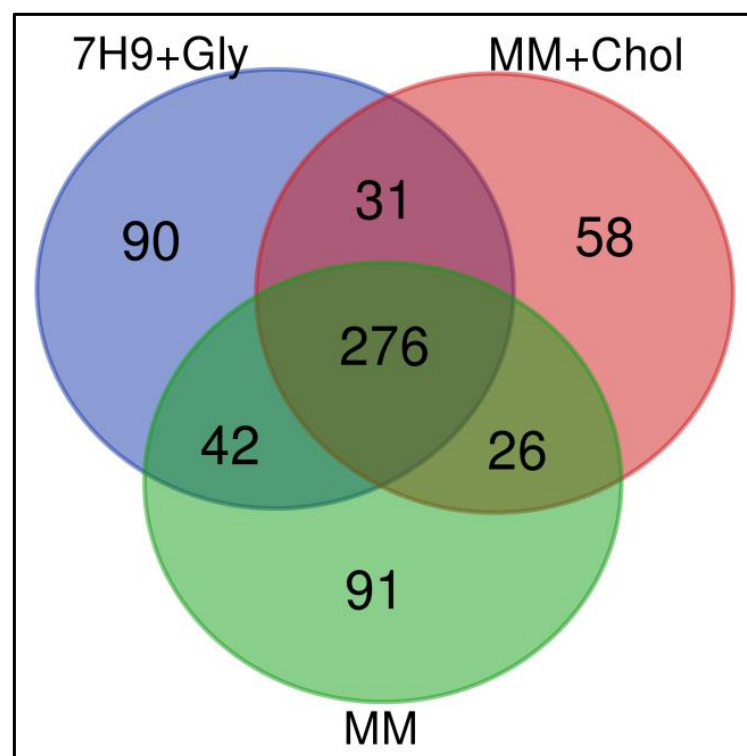


Figure 2. Qualitative analyses of all identified proteins. Venn diagram shows the overlap in the numbers of protein identifications between macrophages infected with *M. smegmatis* after their culture in Middlebrook 7H9 broth (7H9 + Gly), minimal medium with cholesterol supplementation (MM + Chol), and minimal medium without supplementation (MM).

All bacterial groups cultured under the different conditions studied (7H9 + Gly, MM + Chol, and MM) modified the proteome of the infected macrophages J774A.1, when compared with uninfected macrophages. In total, 44 proteins were significantly up or down-regulated in macrophages during infection with *M. smegmatis* grown under different

nutritional conditions, as shown in Table 1. Specifically, 5 proteins were up-regulated and 2 proteins were down-regulated during infection with *M. smegmatis* grown in 7H9 + Gly. In contrast, 7 proteins were up-regulated and 26 proteins were down-regulated during infection by *M. smegmatis* grown in MM + Chol and 4 proteins were up-regulated and no proteins were down-regulated during infection by *M. smegmatis* grown in MM (Table 1). Thus, after cholesterol consumption, mycobacteria significantly influenced the host macrophage proteome, altering the abundance of 33 proteins, which was significantly more than the alterations induced by the 7H9 + Gly and MM groups. The finding that 26 proteins were down-regulated shows that, after cholesterol consumption, mycobacteria can affect several biological processes and molecular functions in the host cell.

Table 1. Quantification of identified, quantified, exclusive, and differentially regulated proteins in proteomic analysis.

| Experimental Groups | Identified Proteins | Quantified Proteins | Exclusive Proteins | Regulated Proteins | |
|---------------------|---------------------|---------------------|--------------------|--------------------|-------|
| | | | | Up- | Down- |
| 7H9 + Gly | 439 | 119 | 90 | 5 | 2 |
| MM + Chol | 391 | 139 | 58 | 7 | 26 |
| MM | 435 | 90 | 91 | 4 | 0 |
| Total | 1265 | | | 44 | |

The identified proteins were cataloged into biological processes (Figure 3A), molecular functions (Figure 3B), and cellular components (Figure 3C). According to GO annotations from the OmicsBox software, ontology reveals that all proteins altered by the three experimental groups were mainly associated with a cellular process, metabolic process, biological regulation, response to stimuli, and others, as shown in Figure 3A. The ontology also showed that these same proteins are mostly associated with transcription regulator activity, transporter activity, molecular function regulators, structural molecule activity, protein binding, and catalytic activity as the chief molecular function, as shown in Figure 3B. All of these biological processes, molecular function, and cellular components have been previously associated with mycobacteria infection [7,21]. This result suggests a complex interaction between the mycobacteria and the host.

3.2. Common Effects—Immune System and Cytoskeleton

Phagocytosis involves cell surface recognition receptors that transmit signals to various cytoskeletal pathways, to initiate the processes of endocytosis, phagocytosis, vesicular trafficking, and autophagy. In this study, proteins associated with the cytoskeleton, immune response, phagocytosis, autophagy, endocytosis, and vesicular transport were altered in all host proteomes (Supplementary Tables). Among the proteins identified after infection of macrophages with *M. smegmatis* grown in 7H9 + Gly, CORO1C and TUBA1C are down-regulated, and NCOR1, PHLDB2, SQSTM1, and IFITM3 are up-regulated (Supplementary Table S1). Only one host protein, IFITM3, was up-regulated by the 7H9 + Gly and MM groups, but not by MM + Chol. Only one cytoskeleton protein, CLASP1, was up-regulated in macrophages infected by *M. smegmatis* grown in MM (Supplementary Table S3). In the MM + Chol group, cytoskeleton and immune proteins such as V-ATPase, PARD3, WDR1, MYH7, PFN1, CFL1, and SEPT2 were down-regulated, and KIF15, VIM, and ANXA3 were up-regulated (Supplementary Table S2).

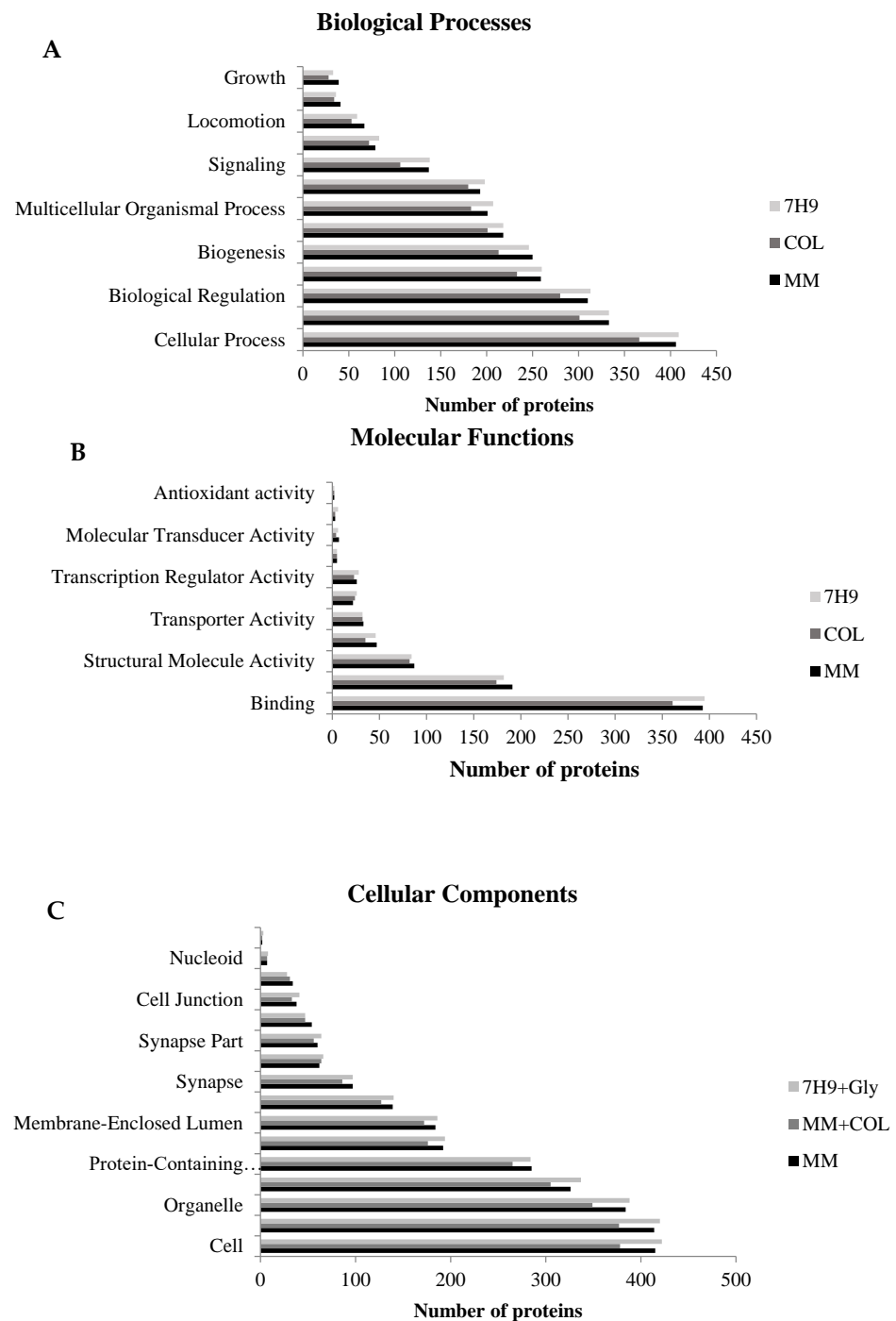


Figure 3. Gene ontology analysis of all identified proteins. Macrophage proteins were analyzed according to their biological process (A), molecular function (B), and cellular component (C). This classification was produced based on an analysis using the Blast2GO Annotation through Omics-Box software.

3.2.1. Cytoskeleton

The cytoskeleton is essential for phagocytosis in immune cells. Infection of macrophages with *M. smegmatis* grown in 7H9 + Gly down-regulated TUBA1C and CORO1C. These proteins are important for cytoskeleton remodeling, protrusion formation, phagocytosis, and the formation of endocytic vesicles [30,31]. Interference in any of these systems leads to multiple defects in vesicular traffic, formation of vesicles, and endosome fission [32]. In fibroblasts, the absence of coronin-1C affects not only actin filaments, but also microtubules and intermediate vimentin filaments, generating deficiency in cell proliferation and migra-

tion [33]. Diaz et al., 2016, also identified CORO1C in exosomes of *M. tuberculosis*-infected cells [21].

In mammals, a function of coronin proteins was initially discovered by studying immune evasion mechanisms used by *M. tuberculosis*. During infection, an important coronin family member, known as TACO or Coronin-1A (CORO-1A), is retained on phagosome macrophages by live mycobacteria to block phagolysosome fusion and thereby prevents the subsequent destruction of the mycobacteria [34,35]. CORO-1A has also been shown to be important for the activation of calcium signaling following mycobacterial entry into macrophages.

The cytoskeleton is involved in all main functions of immune cells related to the response to infection. The architecture of the actin cytoskeleton network is maintained by the coordination of a large number of proteins that regulate the assembly and disassembly of filaments and the contractile force driven by the myosin motor protein. The myosin motor protein can also promote the disassembly of filaments [36]. In the macrophages infected by the MM + Chol group, MYH7, PFN1, CFL1, and WDR1 were all down-regulated. CFL1 and WDR1 are cytoskeleton binding proteins that can work together by inducing the disassembly of actin filaments; their depletion perturbs the actin cytoskeleton [37]. In addition, PFN1 also binds to actin and affects the cytoskeleton structure.

Other cytoskeleton proteins that were up-regulated in macrophages by the MM + Chol *M. smegmatis* group are KIF15, a motor protein of microtubules, ANXA3, and VIM (Vimentine). These last two interact directly and are related to differentiation, migration, phagocytosis, and production of reactive oxygen species [38,39]. VIM is expressed in activated macrophages and responds to pro-inflammatory stimuli [40]. Mahesh et al., 2016, demonstrated that vimentin is up-regulated in macrophages infected with heat-killed *M. tuberculosis* H37Rv and live H37Ra [41]. VIM was also shown to be up-regulated in exosomes of macrophages infected with *M. tuberculosis* [21] and by ManLAM interaction with macrophages [20]. The positive regulation of ANXA3 highlights its role not only as a cytoskeletal protein, but also in blocking the inflammatory process that is inhibited by this protein during infection. ANXA3 blocks phospholipase A2 and consequently prevents the release of arachidonic acid and its modification into prostaglandins and leukotrienes, which are categorized as anti-inflammatory and inflammatory mediators that are important during infection.

3.2.2. Immune System

We analyzed the direct relationship between cytoskeleton proteins, the immune response, and inflammation-related proteins during infection. Previous studies also showed the overexpression of SQSTM1 and IFITM3 in macrophages infected with *M. tuberculosis* [7,20,42]. SQSTM1, up-regulated in the macrophages infected by the 7H9 + Gly group, is one of the best-known substrates for autophagy and participates in selective autophagy; its up-regulation indicates failure in the autophagic process [43,44]. It has been previously shown that phagocytosis is enhanced in autophagy-deficient macrophages, increasing uptake of mycobacteria [43]. IFITM3 was up-regulated in the macrophage infected by the 7H9 + Gly and MM groups; this protein plays a critical role in the structural stability and function of vacuolar ATPase (V-ATPase), a phagosome membrane protein responsible for phagosome acidification and degradation of mycobacteria. IFITM3 restricts mycobacterial growth by mediating endosomal maturation; it acts through interaction with V-ATPase and potentially stabilizes its association with endosomal membranes, increasing the endosomal acidification of cells infected with *M. tuberculosis* [45,46].

In contrast, the MM + Chol *M. smegmatis* group induced different responses in macrophages. After cholesterol consumption, *M. smegmatis* induced down-regulation of V-ATPase, indicating a possible destabilization of this phagosome membrane protein. Previous studies have shown that V-ATPase plays important roles during *M. tuberculosis* infection [6,47,48]. In macrophages, *M. tuberculosis* infection inhibits phagosome acidification by the exclusion of V-ATPase and it is critical for *M. tuberculosis* persistence in host

macrophages [6]. Shui et al., 2011 showed that v-ATPase was down-regulated by ManLAM (Mtb) interaction with macrophages [20]. Thus, the negative regulation of V-ATPase in this experimental group represents an important finding of our study because this is a key protein in phagosome acidification. These results provide further evidence that *M. smegmatis* induced to cholesterol consumption is able to make changes in the host immune response and contributes to phagosome maturation arrest.

All nutritional conditions offered to *M. smegmatis* affect proteins related to cytoskeleton, immune response, and vesicular traffic of the host during infection. Macrophages infected by *M. smegmatis* grown in MM + Chol demonstrated a greater number of affected proteins than those infected by *M. smegmatis* grown in 7H9 + Gly or MM, indicating that, after cholesterol consumption, mycobacteria can modify the response of the host cell and possibly cause failure in the cytoskeleton, which is important for eliminating mycobacteria. Intracellular pathogens subvert the host cytoskeleton to promote their survival, replication, and dissemination. Actin is a common target of bacterial pathogens, but recent studies have also highlighted the targeting of microtubules, cytoskeletal motors, intermediate filaments, and septins. The study of the cytoskeleton during host–pathogen interactions shed light on key cellular processes such as phagocytosis, autophagy, membrane trafficking, motility, and signal transduction [8], while a recent study showed that *M. tuberculosis* lipids modulate macrophage the actin cytoskeleton [9].

3.3. Exclusive Events—Specific Differences in Host Protein Regulation Induced by *M. smegmatis* Infection

3.3.1. Infection of Macrophages by *M. Smegmatis* Grown in 7H9 + Gly up-Regulates CABIN1, a Negative Regulator of Calcineurin

Calcium (Ca^{2+}) is an important factor in the host–pathogen interaction; it plays a significant role in phagocytosis and is involved in cell division, motility, stress response, signaling, amongst other mechanisms. Previous studies suggest that actin filament and cytoskeleton arrangement alterations require several Ca^{2+} -binding proteins/substrates for effective phagocytosis. In the biology of tuberculosis infection, it has been noted that *M. tuberculosis* is able to arrest phagosomal maturation by interfering in Ca^{2+} signaling [49,50].

When macrophages were infected by the 7H9 + Gly group, we identified an exclusive protein that was up-regulated at fold-change 5571 (Supplementary Table S1), known as calcineurin binding protein 1 (CABIN1). CABIN1 inhibits calcineurin, which is a Ca^{2+} - and calmodulin-dependent ser/thr phosphatase. In the presence of calcium influx, calcineurin inhibits the phagosome-lysosome fusion and also acts an actin-binding protein that adheres to the phagosome membrane and prevents the maturation of phagosome-containing bacilli [49,50]. The up-regulation of CABIN1 may favor the host during 7H9 + Gly *M. smegmatis* infection of macrophages by blocking calcineurin and permitting lysosomal delivery of mycobacteria and phagosome-lysosome fusion.

The STRING analysis showed that CABIN1 interacts with other proteins related to cell growth, survival, and apoptosis, DNA repair, replication, transcription, and chromosome segregation (Figure 4A).

3.3.2. Infection of Macrophages with *M. Smegmatis* Grown in MM Induces up-Regulation of CLASP 1, a Cytoskeleton Protein

The microtubule network in mammalian cells is used by a variety of intracellular pathogens to facilitate their uptake and for the formation, stabilization, and maintenance of their intracellular vacuoles. Macrophage infection with *M. smegmatis* grown only in MM medium differentially regulated a protein at fold-change 5096, known CLIP-associating protein 1 (CLASP1), a microtubule plus-end tracking protein that promotes the stabilization of dynamic microtubules. This protein is involved in cellular adhesion, microtubule organization, immune response and promotes the stabilization of dynamic microtubules via their interaction with actin [51]. Zhao et al. (2013) [51] showed that the silencing of CLASP1 in fibroblasts infected with *Trypanosoma cruzi* reduces internalization of the protozoan and delays fusion of CLASP1-depleted vacuoles with the host lysosomes. Here, for the first

time, CLASP1 was related to mycobacterial infection, in the MM group. The up-regulation of CLASP1 may facilitate the internalization of *M. smegmatis* and the phagosome-lysosome fusion in macrophages. These results indicate that *M. smegmatis* cultured in 7H9 + Gly and only in MM may not be able to subvert the immune response of macrophages, which can eliminate the mycobacteria by the positive regulation of two proteins that are related to lysosomal delivery and phagosome-lysosome fusion.

The two differentially-expressed proteins in phagocytes infected with *M. smegmatis* grown in 7H9 + Gly (CABIN1) and MM (CLASP1) were analyzed using STRING-11, with a medium confidence score threshold of 0.4. An interactome network was built for this set of proteins to identify protein-protein interactions and predict functional associations (Figure 4). The STRING analysis of CLASP1 demonstrates its interaction with microtubule cytoskeleton proteins (Figure 4B).

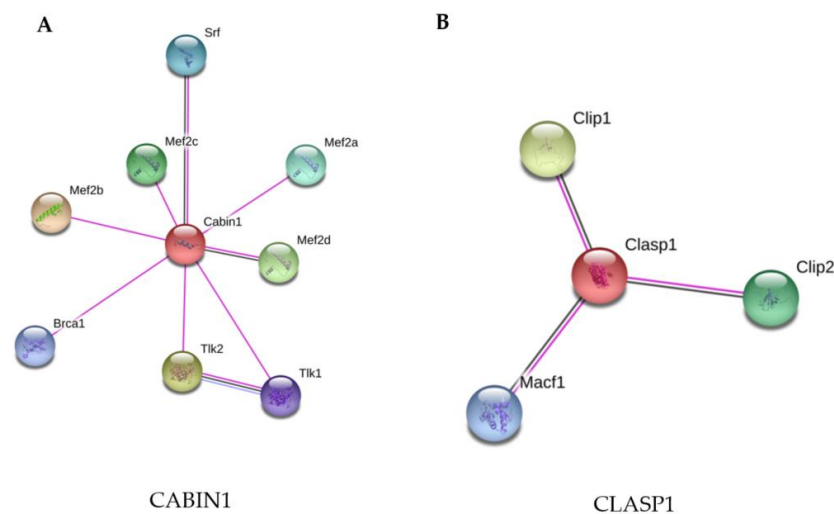


Figure 4. STRING analysis of the CABIN1 and CLASP1 proteins. (A) CABIN1 was up-regulated in macrophages infected with *M. smegmatis* after their culture in Middlebrook 7H9 broth (7H9 + Gly). (B) CLASP1 was up-regulated in macrophages infected with *M. smegmatis* after their culture in minimal medium without supplementation (MM). The proteins were grouped using the STRING software version 11.0. Line colors: known interactions, purple line (determined experimentally); predicted interactions, dark blue (gene co-occurrence); other, black (co-expression).

3.3.3. Infection of Macrophages with *M. smegmatis* Grown in MM + Chol Induces Differential Expression of Proteins of the Immune System and Immunometabolism

In this group, macrophages infected with *M. smegmatis* after cholesterol consumption demonstrated the greatest number of differentially expressed proteins (total of 33). These proteins engage in diverse cellular processes, such as endocytosis and vesicle transport, cytoskeleton rearrangement, ubiquitination pathways, mRNA processing, and immunometabolism. All of these proteins interact with each other, as shown in Figure 5, which suggests a complex interaction between the host and the mycobacteria after cholesterol consumption. Among these proteins, 7 were up-regulated and 26 were down-regulated.

Among the down-regulated proteins, VDAC2 and HSP90 have been reported in other studies of macrophage activation and infection with *M. tuberculosis* [20,52,53]. Patel et al. (2009) showed that HSP90 has a role in the stabilization of the microtubule cytoskeleton during macrophage activation [52]. Other researchers have reported different functions of host Hsp(s) in controlling bacterial infections. During tuberculosis infection, Hsp(s) exhibit different functions, including toll-like receptor (TLR) activation and immune response induction; they also act as a diagnostic tools and may represent potent vaccine candidates [53].

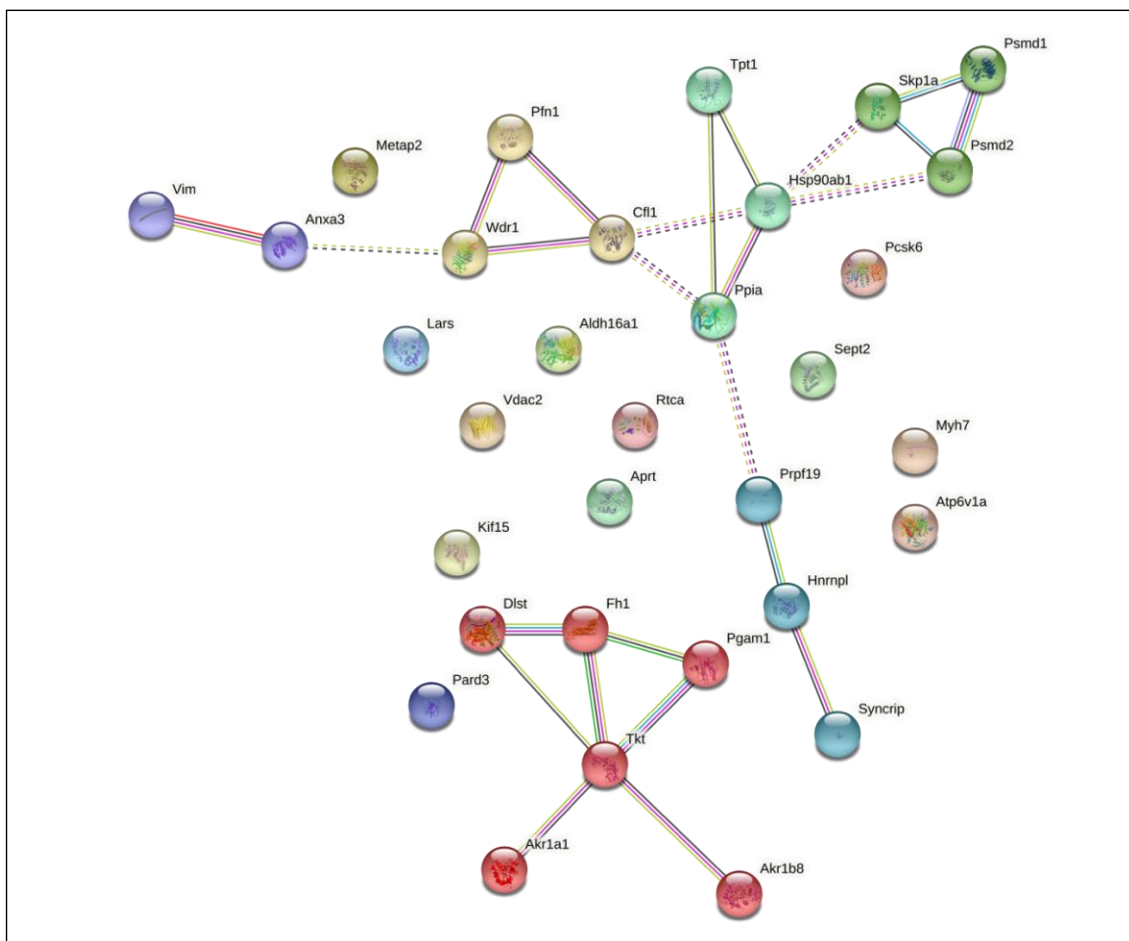


Figure 5. STRING analysis of differentially expressed proteins in macrophages infected with *Mycobacterium smegmatis* after cholesterol consumption (MM + Chol) revealed 20 interaction partners. The proteins were grouped using the STRING software version 11.0. Line colors: known interactions, purple line (determined experimentally); predicted interactions, dark blue (gene co-occurrence); other, black (co-expression).

Interestingly, recent studies have shown that the immune response and metabolic remodeling are interconnected [54]. In response to infection, activation of macrophages makes changes in the bioenergetic pathway from oxidative phosphorylation to glycolysis, and *M. tuberculosis* infection perturbs this pathway to facilitate its survival and persistence [54–58]. Cumming et al. (2018) [58] demonstrated that *M. tuberculosis* induces a quiescent energy phenotype in human monocyte-derived macrophages and decelerated flux through glycolysis and the TCA cycle. Furthermore, *M. tuberculosis* reduced mitochondrial dependency on glucose and increased mitochondrial dependency on fatty acids. A proteomic analysis by Li et al. (2017) [7] demonstrated that, during *M. tuberculosis* infection of THP-1, the most modulated proteins were mainly implicated in metabolic processes important in TB pathogenesis and transmission.

This experimental group demonstrated interference in proteins associated with host metabolism. A total of 11 proteins were differentially regulated; among them, aldo-keto reductase (AKR1A1), aldehyde dehydrogenase (ALDH16A1), aldose reductase (AKR1B8), phosphoglycerate mutase 1 (PGAM1), and transketolase (TKT) were down-regulated and other mitochondrial proteins such dihydrolipoyllysine-residue succinyltransferase (DLST) and fumarate hydratase (FH) were up-regulated. Multiple studies have shown that the perturbation of key metabolic enzymes can affect the immune functions of macrophages [4]. Some metabolic enzymes such as PGAM1, TKT, and ALDH16A1 have also been reported to be associate with the cytoskeleton [52,59].

Microorganisms can modulate the metabolic status of macrophages using virulence factors such as cell wall constituents. Our findings indicate that, after cholesterol consumption, *M. smegmatis* may induce similar responses to *M. tuberculosis* in host proteins, down-regulating glycolytic and redox enzymes, and upregulating mitochondrial enzymes. Among the 33 proteins differentially regulated in macrophages by *M. smegmatis* cultured in MM + Chol, 20 proteins interacted with each other, as shown in Figure 5. ANXA3, a member of the calcium-dependent phospholipid-binding protein family that inhibits the function of phospholipase A2, interacted with VIM which integrates the cytoskeleton. ANXA3 also interacts with WDR1, an actin-binding protein that interacts with other cytoskeleton proteins such as PFN1 and CFL1, demonstrating the direct relationship between the cytoskeleton and the immune response. Other proteins, for instance HSP90, TPT1, SKP1A, PSMD1, PSMD2, and PPIA, are related to protein folding, stabilization, and degradation. PRPF19, HNRNPL, and SYNCRIP are related to mRNA processing. Six proteins, DLST, FH1, PGAM1, TKT, AKR1A1, and AKR1B8, which are involved in immunometabolism, show interactions with each other.

4. Conclusions

The alterations of different biological processes in macrophages after infection with *M. smegmatis* grown in different nutritional conditions helps us to understand that, when bacilli use the carbon source available in the environment, this modifies their metabolism and induces different macrophage responses. In particular, cholesterol consumption by *M. smegmatis* grown in MM causes several changes in cell wall bioactive components. We hypothesized that cholesterol-modified bioactive molecules may be interacting with macrophages to down-regulate many proteins involved in key biological processes within the cell. Thus, *M. smegmatis* could be modulating the immune response to remain viable within the host.

During macrophage infection with *M. smegmatis* cultured in 7H9 + Gly complete medium, only 7 proteins related to the cytoskeleton, vesicular traffic, and immune response were differentially regulated. In this group, most proteins presented up-regulation (e.g., SQSTM1, IFITM3, NCOR1, PHLDB2, and CABIN1), indicating enhancement of phagocytosis, stabilization of the V-ATPase phagosome protein, endosomal acidification, and favoring of phagosome-lysosome fusion. Similarly, macrophages infected with *M. smegmatis* grown in MM without any supplementation induced only up-regulation of proteins such as IFITM3 and CLASP1, indicating that macrophages are able to eliminate mycobacteria by the positive regulation of proteins related to the stabilization of the phagosome and dynamic microtubules, allowing lysosomal delivery and phagosome-lysosome fusion.

In contrast, the most interesting results in our study were observed for macrophages infected with *M. smegmatis* that were cultured in MM + Chol. Here, mycobacterial infection induced greater differential expression of proteins. Of the 33 differentially expressed proteins, 26 were down-regulated, including V-ATPase, VDAC2, HSP90, TPT1, PPIA, PARD3, MYH7, PFN1, WDR1, CFL1, SEPT2, METAP2, APRT, LARS, TKT, PGAM1, AKR1A1, ALDH16A1, and AKR1B8. These proteins are related to several biological processes such as cytoskeleton remodeling, the ubiquitination pathway, immune response, mRNA processing, and immunometabolism. Our data reveal that, after cholesterol consumption, the mycobacteria interact with macrophages in a more complex way, down-regulating diverse proteins that are important for cytoskeleton remodeling, an essential biological process for phagocytosis and endocytosis. In addition, negative regulation of V-ATPase indicates interference in phagosome acidification, as occurs during *M. tuberculosis* infection. Another important finding of this study was the down-regulation of immunometabolism proteins that have recently been found to be important for the host–pathogen interaction. Recent studies have reported that *M. tuberculosis* causes metabolic remodeling of immune cells to facilitate its survival and to persist in the host [55]. Here, the saprophytic *M. smegmatis*, following cholesterol consumption, is able to perturb macrophage proteins involved in metabolism, similarly to *M. tuberculosis*. Santos et al., 2019, showed that *M. smegmatis*,

grown in MM medium with cholesterol supplementation, demonstrates changes in its bioactive cell wall components, cell surface hydrophobicity, acquires H₂O₂ resistance, and presents granuloma like-structure formation [16]. Thus, these results indicate that the modification of bioactive cell wall molecules of *M. smegmatis* by cholesterol consumption may modulate the immune response of macrophages through down-regulation of key proteins related to the biological processes of the immune response, immunometabolism and cytoskeleton remodeling. As such, these bacterial may be able to subvert the defense mechanisms of macrophages to facilitate their survival inside the host.

In conclusion, our study provides the first proteomic analysis that compares a large number of cellular proteins that are differentially regulated in macrophages by *M. smegmatis*, after inducing cholesterol consumption or not. The dynamic responses to infection caused by these mycobacteria are also characterized. This information will be important for understanding how mycobacteria use the carbon source available in the environment to manipulate the metabolism and defense mechanisms of the host macrophage. A more comprehensive understanding of host–pathogen interaction, cellular metabolism, and signaling networks may provide a novel avenue to improve disease therapeutics, vaccines, and biomarkers for *M. tuberculosis* infection. Furthermore, understanding how microbial metabolism interacts with macrophage metabolism and how this influences the control or progression of infection may shape future investigations.

Supplementary Materials: The following are available online at <https://www.mdpi.com/article/10.3390/pathogens10060662/s1>, Table S1: List of differentially regulated proteins from the group of macrophages infected with *M. smegmatis* grown in complete 7H9 medium supplemented with glycerol (7H9 + Glycerol); Table S2: List of differentially regulated proteins from the group of macrophages infected with *M. smegmatis* grown in minimal medium supplemented with cholesterol (MM + Cholesterol); Table S3: List of differentially regulated proteins from the group of macrophages infected with *M. smegmatis* grown in minimal medium without supplementation (MM).

Author Contributions: Conceptualization, C.B.C.d.S., A.V.S. and J.B.d.L.; methodology, C.B.C.d.S., A.V.S., J.B.d.L., J.S.C., L.P.d.S.F. and R.B.d.S.V.; software, J.B.d.L. and J.S.C. formal analysis, C.B.C.d.S., A.V.S. and J.B.d.L.; investigation, C.B.C.d.S., A.V.S. and J.B.d.L.; resources, C.B.C.d.S., A.V.S., L.P.X., B.d.M.M., E.O.d.S., R.B.d.S.V. and J.L.M.d.N.; writing—original draft preparation, J.B.d.L.; writing—review and editing, J.B.d.L. and J.S.C.; supervision, C.B.C.d.S., A.V.S., J.S.C., L.P.X., B.d.M.M., E.O.d.S., R.B.d.S.V. and J.L.M.d.N.; All authors have read and agreed to the published version of the manuscript.

Funding: This study was financed in part by Coordenação de Aperfeiçoamento de Pessoal de Nível Superior—Brasil (CAPES)—Finance Code 001.

Institutional Review Board Statement: Not applicable.

Informed Consent Statement: Not applicable.

Data Availability Statement: The mass spectrometry proteomics data have been deposited at the ProteomeXchange Consortium via the PRIDE partner repository with the dataset identifier PXD025783.

Acknowledgments: The authors would like to thank Pró-Reitoria de Pesquisa e Pós-Graduação da Universidade Federal do Pará (PROPESP/UFGA).

Conflicts of Interest: The authors declare no conflict of interest.

References

1. World Health Organization. *Global Tuberculosis Report 2020*; World Health Organization: Geneva, Switzerland, 2020.
2. VanderVen, B.C.; Huang, L.; Rohde, K.H.; Russell, D.G. The Minimal Unit of Infection: Mycobacterium tuberculosis in the Macrophage. *Microbiol. Spectr.* **2016**, *4*. [CrossRef]
3. Hmama, Z.; Peña-Díaz, S.; Joseph, S.; Av-Gay, Y. Immuno-evasion and immunosuppression of the macrophage by *Mycobacterium tuberculosis*. *Immunol. Rev.* **2015**, *264*, 220–232. [CrossRef]
4. Russell, D.G.; Huang, L.; VanderVen, B.C. Immunometabolism at the interface between macrophages and pathogens. *Nat. Rev. Immunol.* **2019**, *19*, 291–304. [CrossRef] [PubMed]

5. Armstrong, J.A.; Hart, P.D. Phagosome-lysosome interactions in cultured macrophages infected with virulent tubercle bacilli. Reversal of the usual nonfusion pattern and observations on bacterial survival. *J. Exp. Med.* **1975**, *142*, 1–16. [[CrossRef](#)]
6. Sturgill-Koszycki, S.S.; Chakraborty, P.; Haddix, P.L.; Collins, H.L.; Russell, D.G. Lack of Acidification in Mycobacterium Phagosomes Produced by Exclusion of the Vesicular Proton-ATPase. *Science* **1994**, *263*, 4. [[CrossRef](#)]
7. Li, P.; Wang, R.; Dong, W.; Hu, L.; Zong, B.; Zhang, Y.; Wang, X.; Guo, A.; Zhang, A.; Xiang, Y.; et al. Comparative Proteomics Analysis of Human Macrophages Infected with Virulent Mycobacterium bovis. *Front. Cell. Infect. Microbiol.* **2017**, *7*, 15. [[CrossRef](#)]
8. Haglund, C.M.; Welch, M.D. Pathogens and polymers: Microbe–host interactions illuminate the cytoskeleton. *J. Cell Biol.* **2011**, *195*, 7–17. [[CrossRef](#)]
9. Mishra, M.; Dadhich, R.; Mogha, P.; Kapoor, S. Mycobacterium Lipids Modulate Host Cell Membrane Mechanics, Lipid Diffusivity, and Cytoskeleton in a Virulence-Selective Manner. *ACS Infect. Dis.* **2020**, *6*, 2386–2399. [[CrossRef](#)]
10. He, Y.; Li, W.; Liao, G.; Xie, J. Mycobacterium tuberculosis -Specific Phagosome Proteome and Underlying Signaling Pathways. *J. Proteome Res.* **2012**, *11*, 2635–2643. [[CrossRef](#)]
11. Anes, E.; Peyron, P.; Staali, L.; Jordao, L.; Gutierrez, M.G.; Kress, H.; Hagedorn, M.; Maridonneau-Parini, I.; Skinner, M.A.; Wildeman, A.G.; et al. Dynamic life and death interactions between Mycobacterium smegmatis and J774 macrophages. *Cell. Microbiol.* **2006**, *8*, 939–960. [[CrossRef](#)]
12. Jordao, L.; Bleck, C.K.E.; Mayorga, L.; Griffiths, G.; Anes, E. On the killing of mycobacteria by macrophages. *Cell. Microbiol.* **2007**, *10*, 529–548. [[CrossRef](#)] [[PubMed](#)]
13. Pandey, A.K.; Sasseti, C.M. Mycobacterial persistence requires the utilization of host cholesterol. *Proc. Natl. Acad. Sci. USA* **2008**, *105*, 4376–4380. [[CrossRef](#)] [[PubMed](#)]
14. Griffin, J.E.; Pandey, A.K.; Gilmore, S.A.; Mizrahi, V.; McKinney, J.D.; Bertozzi, C.R.; Sasseti, C.M. Cholesterol Catabolism by Mycobacterium tuberculosis Requires Transcriptional and Metabolic Adaptations. *Chem. Biol.* **2012**, *19*, 218–227. [[CrossRef](#)]
15. Lovewell, R.R.; Sasseti, C.M.; VanderVen, B.C. Chewing the fat: Lipid metabolism and homeostasis during M. tuberculosis infection. *Curr. Opin. Microbiol.* **2016**, *29*, 30–36. [[CrossRef](#)]
16. Dos Santos, A.C.D.; Marinho, V.H.D.S.; Silva, P.H.D.A.; Macchi, B.D.M.; Arruda, M.S.P.; Da Silva, E.O.; Nascimento, J.L.M.D.; De Sena, C.B.C. Microenvironment of Mycobacterium smegmatis Culture to Induce Cholesterol Consumption Does Cell Wall Remodeling and Enables the Formation of Granuloma-Like Structures. *BioMed Res. Int.* **2019**, *2019*, 1–13. [[CrossRef](#)]
17. Brzostek, A.; Pawelczyk, J.; Rumijowska-Galewicz, A.; Dziadek, B.; Dziadek, J. Mycobacterium tuberculosis Is Able To Accumulate and Utilize Cholesterol. *J. Bacteriol.* **2009**, *191*, 6584–6591. [[CrossRef](#)]
18. Li, H.; Wei, S.; Fang, Y.; Li, M.; Li, X.; Li, Z.; Zhang, J.; Zhu, G.; Li, C.; Bi, L.; et al. Quantitative proteomic analysis of host responses triggered by Mycobacterium tuberculosis infection in human macrophage cells. *Acta Biochim. Biophys. Sin.* **2017**, *49*, 835–844. [[CrossRef](#)]
19. Shui, W.; Gilmore, S.A.; Sheu, L.; Liu, J.; Keasling, J.D.; Bertozzi, C.R. Quantitative Proteomic Profiling of Host–Pathogen Interactions: The Macrophage Response to Mycobacterium tuberculosis Lipids. *J. Proteome Res.* **2009**, *8*, 282–289. [[CrossRef](#)]
20. Shui, W.; Petzold, C.J.; Redding, A.; Liu, J.; Pitcher, A.; Sheu, L.; Hsieh, T.-Y.; Keasling, J.D.; Bertozzi, C.R. Organelle Membrane Proteomics Reveals Differential Influence of Mycobacterial Lipoglycans on Macrophage Phagosome Maturation and Autophagosome Accumulation. *J. Proteome Res.* **2011**, *10*, 339–348. [[CrossRef](#)]
21. Diaz, G.; Wolfe, L.M.; Kruh-Garcia, N.A.; Dobos, K.M. Changes in the Membrane-Associated Proteins of Exosomes Released from Human Macrophages after Mycobacterium tuberculosis Infection. *Sci. Rep.* **2016**, *6*, 1–10. [[CrossRef](#)]
22. Menon, D.; Singh, K.; Pinto, S.M.; Nandy, A.; Jaisinghani, N.; Kutum, R.; Dash, D.; Prasad, T.S.K.; Gandotra, S. Quantitative Lipid Droplet Proteomics Reveals Mycobacterium tuberculosis Induced Alterations in Macrophage Response to Infection. *ACS Infect. Dis.* **2019**, *5*, 559–569. [[CrossRef](#)]
23. Sena, C.B.C.; Fukuda, T.; Miyahagi, K.; Matsumoto, S.; Kobayashi, K.; Murakami, Y.; Maeda, Y.; Kinoshita, T.; Morita, Y.S. Controlled expression of branch-forming mannosyltransferase is critical for mycobacterial lipoarabinomannan biosynthesis. *J. Biol. Chem.* **2010**, *285*, 13326–13336. [[CrossRef](#)] [[PubMed](#)]
24. Cassoli, J.S.; Martins-De-Souza, D. *Comprehensive Shotgun Proteomic Analyses of Oligodendrocytes Using Ion Mobility and Data-Independent Acquisition*; Springer Nature Experiments, 2017; Volume 127, Available online: https://experiments.springernature.com/articles/10.1007/978-1-4939-7119-0_5 (accessed on 20 July 2020).
25. Nascimento, S.V.D.; Magalhães, M.M.; Cunha, R.L.; Costa, P.H.D.O.; Alves, R.C.D.O.; De Oliveira, G.C.; Valadares, R.B.D.S. Differential accumulation of proteins in oil palms affected by fatal yellowing disease. *PLoS ONE* **2018**, *13*, e0195538. [[CrossRef](#)] [[PubMed](#)]
26. Li, G.-Z.; Vissers, J.P.C.; Silva, J.C.; Golick, D.; Gorenstein, M.V.; Geromanos, S.J. Database searching and accounting of multiplexed precursor and product ion spectra from the data independent analysis of simple and complex peptide mixtures. *Proteomics* **2009**, *9*, 1696–1719. [[CrossRef](#)] [[PubMed](#)]
27. Deutsch, E.W.; Bandeira, N.; Sharma, V.; Perez-Riverol, Y.; Carver, J.J.; Kundu, D.J.; García-Seisdedos, D.; Jarnuczak, A.F.; Hewapathirana, S.; Pullman, B.S.; et al. The ProteomeXchange consortium in 2020: Enabling ‘big data’ approaches in proteomics. *Nucleic Acids Res.* **2020**, *48*, 1145–1152. [[CrossRef](#)]
28. Perez-Riverol, Y.; Xu, Q.-W.; Wang, R.; Uszkoreit, J.; Griss, J.; Sanchez, A.; Reisinger, F.; Csordas, A.; Ternent, T.; Del-Toro, N.; et al. PRIDE Inspector Toolsuite: Moving Toward a Universal Visualization Tool for Proteomics Data Standard Formats and Quality Assessment of ProteomeXchange Datasets. *Mol. Cell. Proteom.* **2016**, *15*, 305–317. [[CrossRef](#)]

29. Perez-Riverol, Y.; Csordas, A.; Bai, J.; Bernal-Llinares, M.; Hewapathirana, S.; Kundu, D.J.; Inuganti, A.; Griss, J.; Mayer, G.; Eisenacher, M.; et al. The PRIDE database and related tools and resources in 2019: Improving support for quantification data. *Nucleic Acids Res.* **2019**, *47*, D442–D450. [[CrossRef](#)]
30. Rosentreter, A.; Hofmann, A.; Xavier, C.-P.; Stumpf, M.; Noegel, A.A.; Clemen, C.S. Coronin 3 involvement in F-actin-dependent processes at the cell cortex. *Exp. Cell Res.* **2007**, *313*, 878–895. [[CrossRef](#)]
31. Rybakina, V.; Clemen, C.S. Coronin proteins as multifunctional regulators of the cytoskeleton and membrane trafficking. *Bioessays* **2005**, *27*, 625–632. [[CrossRef](#)]
32. Hoyer, M.J.; Chitwood, P.J.; Ebmeier, C.C.; Striepen, J.F.; Qi, R.Z.; Old, W.M.; Voeltz, G.K. A Novel Class of ER Membrane Proteins Regulates ER-Associated Endosome Fission. *Cell* **2018**, *175*, 254–265. [[CrossRef](#)]
33. Behrens, J.; Solga, R.; Ziemann, A.; Rastetter, R.H.; Berwanger, C.; Herrmann, H.; Noegel, A.A.; Clemen, C.S. Coronin 1C-free primary mouse fibroblasts exhibit robust rearrangements in the orientation of actin filaments, microtubules and intermediate filaments. *Eur. J. Cell Biol.* **2016**, *95*, 239–251. [[CrossRef](#)]
34. Pieters, J.; Müller, P.; Jayachandran, R. On guard: Coronin proteins in innate and adaptive immunity. *Nat. Rev. Immunol.* **2013**, *13*, 1–9. [[CrossRef](#)]
35. Mori, M.; Mode, R.; Pieters, J. From Phagocytes to Immune Defense: Roles for Coronin Proteins in Dictyostelium and Mammalian Immunity. *Front. Cell. Infect. Microbiol.* **2018**, *8*, 77. [[CrossRef](#)]
36. Reymann, A.-C.; Boujemaa-Paterski, R.; Martiel, J.-L.; Guérin, C.; Cao, W.; Chin, H.F.; De La Cruz, E.M.; Théry, M.; Blanchoin, L. Actin Network Architecture Can Determine Myosin Motor Activity. *Science* **2012**, *336*, 1310–1314. [[CrossRef](#)] [[PubMed](#)]
37. Luxenburg, C.; Heller, E.; Pasolli, H.A.; Chai, S.; Nikolova, M.; Stokes, N.; Fuchs, E. Wdr1-mediated cell shape dynamics and cortical tension are essential for epidermal planar cell polarity. *Nat. Cell Biol.* **2015**, *17*, 592–604. [[CrossRef](#)] [[PubMed](#)]
38. Rius, C.; Aller, P. Vimentin expression as a late event in the in vitro differentiation of human promonocytic cells. *J. Cell Sci.* **1992**, *101*, 395–401. [[CrossRef](#)] [[PubMed](#)]
39. Beneš, P.; Macečková, V.; Zdráhal, Z.; Konečná, H.; Zahradníčková, E.; Mužík, J.; Šmarda, J. Role of vimentin in regulation of monocyte/macrophage differentiation. *Differentiation* **2006**, *74*, 265–276. [[CrossRef](#)] [[PubMed](#)]
40. Mor-Vaknin, N.; Punturieri, A.; Sitwala, K.; Markovitz, D.M. Vimentin is secreted by activated macrophages. *Nat. Cell Biol.* **2003**, *5*, 59–63. [[CrossRef](#)] [[PubMed](#)]
41. Mahesh, P.P.; Retnakumar, R.J.; Mundayoor, S. Downregulation of vimentin in macrophages infected with live Mycobacterium tuberculosis is mediated by Reactive Oxygen Species. *Sci. Rep.* **2016**, *6*, 1–12. [[CrossRef](#)]
42. Hare, N.J.; Chan, B.; Chan, E.; Kaufman, K.L.; Britton, W.J.; Saunders, B.M. Microparticles released from Mycobacterium tuberculosis-infected human macrophages contain increased levels of the type I interferon inducible proteins including ISG15. *Proteomics* **2015**, *15*, 3020–3029. [[CrossRef](#)] [[PubMed](#)]
43. Bonilla, D.L.; Bhattacharya, A.; Sha, Y.; Xu, Y.; Xiang, Q.; Kan, A.; Jagannath, C.; Komatsu, M.; Eissa, N.T. Autophagy Regulates Phagocytosis by Modulating the Expression of Scavenger Receptors. *Immunity* **2013**, *39*, 537–547. [[CrossRef](#)]
44. Bjørkøy, G.; Lamark, T.; Johansen, T. p62/SQSTM1: A Missing Link between Protein Aggregates and the Autophagy Machinery. *Autophagy* **2006**, *2*, 138–139. [[CrossRef](#)]
45. Wee, Y.S.; Roundy, K.M.; Weis, J.J.; Weis, J.H. Interferon-inducible transmembrane proteins of the innate immune response act as membrane organizers by influencing clathrin and v-ATPase localization and function. *Innate Immun.* **2012**, *18*, 834–845. [[CrossRef](#)]
46. Ranjbar, S.; Haridas, V.; Jasenosky, L.D.; Falvo, J.V.; Goldfeld, A.E. A Role for IFITM Proteins in Restriction of Mycobacterium tuberculosis Infection. *Cell Rep.* **2015**, *13*, 874–883. [[CrossRef](#)]
47. Wong, D.; Bach, H.; Sun, J.; Hmama, Z.; Av-Gay, Y. Mycobacterium tuberculosis protein tyrosine phosphatase (PtpA) excludes host vacuolar-H⁺-ATPase to inhibit phagosome acidification. *Proc. Natl. Acad. Sci. USA* **2011**, *108*, 19371–19376. [[CrossRef](#)] [[PubMed](#)]
48. Wong, D.; Li, W.; Chao, J.D.; Zhou, P.; Narula, G.; Tsui, C.; Ko, M.; Xie, J.; Martinez-Frailes, C.; Av-Gay, Y. Protein tyrosine kinase, PtkA, is required for Mycobacterium tuberculosis growth in macrophages. *Sci. Rep.* **2018**, *8*, 155. [[CrossRef](#)] [[PubMed](#)]
49. Sharma, S.; Meena, L.S. Potential of Ca²⁺ in Mycobacterium tuberculosis H37Rv Pathogenesis and Survival. *Appl. Biochem. Biotechnol.* **2016**, *181*, 762–771. [[CrossRef](#)] [[PubMed](#)]
50. Meena, L.S. Interrelation of Ca²⁺ and PE_PGRS proteins during Mycobacterium tuberculosis pathogenesis. *J. Biosci.* **2019**, *44*, 24. [[CrossRef](#)]
51. Zhao, X.; Kumar, P.; Shah-Simpson, S.; CaraDonna, K.L.; Galjart, N.; Teygong, C.; Blader, I.; Wittmann, T.; Burleigh, B.A. Host microtubule plus-end binding protein CLASP1 influences sequential steps in the *Trypanosoma cruzi* infection process: Microtubule plus-end binding proteins facilitate intracellular trypanosome infection. *Cell. Microbiol.* **2013**, *15*, 571–584. [[CrossRef](#)]
52. Patel, P.C.; Fisher, K.H.; Yang, E.C.C.; Harrison, R.E. Proteomic Analysis of Microtubule-associated Proteins during Macrophage Activation. *Mol. Cell. Proteom.* **2009**, *8*, 2500–2514. [[CrossRef](#)] [[PubMed](#)]
53. Shekhawat, S.D.; Purohit, H.J.; Taori, G.M.; Daginawala, H.F.; Kashyap, R.S. Evaluation of heat shock proteins for discriminating between latent tuberculosis infection and active tuberculosis: A preliminary report. *J. Infect. Public Health* **2016**, *9*, 143–152. [[CrossRef](#)] [[PubMed](#)]
54. Kumar, R.; Singh, P.; Kolloli, A.; Shi, L.; Bushkin, Y.; Tyagi, S.; Subbian, S. Immunometabolism of Phagocytes During Mycobacterium tuberculosis Infection. *Front. Mol. Biosci.* **2019**, *6*, 105. [[CrossRef](#)] [[PubMed](#)]
55. Shi, L.; Eugenin, E.A.; Subbian, S. Immunometabolism in Tuberculosis. *Front. Immunol.* **2016**, *7*. [[CrossRef](#)] [[PubMed](#)]

56. Shi, L.; Jiang, Q.; Bushkin, Y.; Subbian, S.; Tyagi, S. Biphasic Dynamics of Macrophage Immunometabolism during *Mycobacterium tuberculosis* Infection. *mBio* **2019**, *10*, e02550-18. [[CrossRef](#)]
57. Shi, L.; Salamon, H.; Eugenin, E.A.; Pine, R.; Cooper, A.; Gennaro, M.L. Infection with *Mycobacterium tuberculosis* induces the Warburg effect in mouse lungs. *Sci. Rep.* **2016**, *5*, 18176. [[CrossRef](#)] [[PubMed](#)]
58. Cumming, B.M.; Addicott, K.W.; Adamson, J.H.; Steyn, A.J. *Mycobacterium tuberculosis* induces decelerated bioenergetic metabolism in human macrophages. *eLife* **2018**, *7*, 1–18. [[CrossRef](#)]
59. Radulovic, M.; Godovac-Zimmermann, J. Proteomic approaches to understanding the role of the cytoskeleton in host-defense mechanisms. *Expert Rev. Proteom.* **2011**, *8*, 117–126. [[CrossRef](#)]